ORIGINAL ARTICLE

Cancer Science WILEY

Long noncoding RNA OVAAL enhances nucleotide synthesis through pyruvate carboxylase to promote 5-fluorouracil resistance in gastric cancer

Jia-nan Tan[1] | Sheng-ning Zhou[1] | Wei Zhang[2] | Bin Yang[1] | Guang-yu Zhong[1] | Jing Huang[1] | Hai Hu[2] | Fang-hai Han[1] | Man-Li Luo[3,4] (ORCID)

[1]Department of Gastrointestinal Surgery, Sun Yat-Sen Memorial Hospital, Sun Yat-Sen University, Guangzhou, China

[2]Department of Oncology, Sun Yat-Sen Memorial Hospital, Sun Yat-Sen University, Guangzhou, China

[3]Medical Research Center, Sun Yat-Sen Memorial Hospital, Sun Yat-Sen University, Guangzhou, China

[4]Guangdong Provincial Key Laboratory of Malignant Tumor Epigenetics and Gene Regulation, Guangdong-Hong Kong Joint Laboratory for RNA Medicine, Sun Yat-Sen Memorial Hospital, Sun Yat-Sen University, Guangzhou, China

Correspondence
Fang-hai Han, Department of Gastrointestinal Surgery, Sun Yat-Sen Memorial Hospital, Sun Yat-Sen University, 107 Yan Jiang West Road, Guangzhou 510120, China.
Email: fh_han@163.com

Man-Li Luo, Medical Research Center, Sun Yat-Sen Memorial Hospital, Sun Yat-Sen University, 107 Yan Jiang West Road, Guangzhou 510120, China.
Email: luomli@mail.sysu.edu.cn

Abstract

5-Fluorouracil (5-FU) is widely used in gastric cancer treatment, yet 5-FU resistance remains an important clinical challenge. We established a model based on five long noncoding RNAs (lncRNA) to effectively assess the prognosis of gastric cancer patients; among them, lncRNA OVAAL was markedly upregulated in gastric cancer and associated with poor prognosis and 5-FU resistance. In vitro and in vivo assays confirmed that OVAAL promoted proliferation and 5-FU resistance of gastric cancer cells. Mechanistically, OVAAL bound with pyruvate carboxylase (PC) and stabilized PC from HSC70/CHIP-mediated ubiquitination and degradation. OVAAL knockdown reduced intracellular levels of oxaloacetate and aspartate, and the subsequent pyrimidine synthesis, which could be rescued by PC overexpression. Moreover, OVAAL knockdown increased sensitivity to 5-FU treatment, which could be reversed by PC overexpression or repletion of oxaloacetate, aspartate, or uridine. OVAAL overexpression enhanced pyrimidine synthesis to promote proliferation and 5-FU resistance of gastric cancer cells, which could be abolished by PC knockdown. Thus, OVAAL promoted gastric cancer cell proliferation and induced 5-FU resistance by enhancing pyrimidine biosynthesis to antagonize 5-FU induced thymidylate synthase dysfunction. Targeting OVAAL-mediated nucleotide metabolic reprograming would be a promising strategy to overcome chemoresistance in gastric cancer.

Jia-nan Tan, Sheng-ning Zhou, and Wei Zhang contributed equally to this work.

1 | INTRODUCTION

Gastric cancer is the third most common cause of cancer-related death worldwide.[1,2] Chemotherapy of GC is based on combination with fluorouracil. Despite advances in surgical treatment, the survival rates of GC have not been effectively improved, which is mainly related to intrinsic or acquired chemoresistance.[3] The underlying molecular mechanisms of GC progression and chemoresistance are largely unclear. Thus, there is an urgent need to gain an in-depth understanding of the molecular mechanisms of GC tumorigenesis and chemoresistance.

Long noncoding RNAs are a class of noncoding transcripts longer than 200 nucleotides in length and have been shown to regulate several crucial biological functions.[4–6] Mechanistically, lncRNA regulates these cellular processes by interacting with and regulating macromolecules, including DNA, RNA, and proteins.[7] Increasing evidence has shown that lncRNAs influence tumorigenesis and cancer progression and drug resistance. For example, the lncRNAs HOTAIR, MALAT1, and GAS5 are considered to play important roles in tumor initiation and development.[8–10] Long noncoding RNA CRAL acts as competing endogenous RNA to decrease cisplatin resistance of GC through the microRNA-505/CYLD/AKT axis.[11] Our group revealed that lncRNA BDNF-AS promoted endocrine resistance of breast cancers by activating mTOR signaling.[12] However, lncRNAs that regulate chemoresistance in GC are still largely unknown.

Metabolic reprograming is a hallmark of cancer.[13] Long noncoding RNAs reprogram cancer metabolism by modulating the key metabolic regulators. Our previous study discovered that lncRNA HIFAL and HISLA drove hypoxia-inducible factor-1α mediated transactivation and glycolysis.[14,15] Metabolic reprograming not only drives cancer development but also chemoresistance of cancers. Our group revealed that activation of nonoxidative pentose phosphate pathway in breast cancer induced chemoresistance.[16] JAK/STAT3 transcriptionally upregulates CPT1B to enhance the fatty acid β-oxidation, which promotes chemoresistance by regulating breast CSCs.[17] DECR1 regulated redox homeostasis by balancing intracellular levels of saturated and unsaturated phospholipids to participate in the resistance of androgen receptor antagonist in prostate cancer.[18]

In the present study, we undertook a bioinformatics analysis of the TCGA GC dataset and identified the lncRNA OVAAL, whose overexpression was associated with poor outcome of GC patients and resistance to 5-FU treatment. We further revealed that OVAAL prevented proteasomal degradation of PC, thus accelerated the production of oxaloacetate from pyruvate and the following accumulation of malate and aspartate, which enhanced the pyrimidine production for cell proliferation. We found that OVAAL overexpressed GC cells were more resistance to 5-FU-induced pyrimidine metabolism abnormalities and thus become resistance to 5-FU treatment.

2 | MATERIALS AND METHODS

2.1 | Patients and clinical samples

Thirty-four primary GC samples and paired nontumor samples (cohort 1) were collected from patients at Sun Yat-Sen Memorial Hospital from January 2015 to January 2016. One hundred and twenty primary GC samples with clinicopathologic data and prognosis data (cohort 2) were collected from GC patients who underwent surgery at Sun Yat-Sen Memorial Hospital from January 2010 to January 2015. The nontumor samples were collected at least 5 cm from the tumor.

2.2 | Bioinformatics analysis

RNA sequencing and corresponding clinical data of GC patients were obtained from the public TCGA database. In total, 1978 lncRNAs were identified by differential expression analysis between the tumor and normal tissues (log2|fold change|> 1 and p-value <0.05). We further undertook univariable Cox regression analysis to identify prognosis-related lncRNAs. We ranked these candidate lncRNAs by p-value of univariable Cox regression for subsequent analysis. We then constructed an lncRNA-based risk score model by considering each lncRNA's HR and AIC. Finally, five lncRNAs were used for establishing a risk score model and calculated their risk score using the following formula:

$$\text{Risk score} = \sum_{i=0}^{n} \text{Coef}_i \, \beta_i,$$

in which Coef_i and β_i represent the coefficient of the multivariate regression Cox analysis and expression level of each lncRNA, respectively. We used the median score as the cut-off value to divide patients into high- and low-risk groups; survival analysis and ROC curves were applied to evaluate this risk model. All the analyses were carried out using R 3.5.2.

2.3 | Animal experiment

To evaluate the effects of OVAAL knockdown and PC overexpression under OVAAL knockdown on tumorigenicity and 5-FU therapy in vivo, 5×10^6 BGC823 cells expressing shCtrl or shOVAAL1/2 and 5×10^6 shOVAAL BGC823 cells transfected with vector or pcDNA3.1-PC were subcutaneously injected into the right dorsal flank of 4-week-old male BALB/C nude mice (Vital River). Intraperitoneal injection of either 5-FU (15 mg/kg) or PBS was carried out every 3 days.

2.4 | RNA pull-down assays and mass spectrometry analyses

In vitro, 3 μg biotinylated RNAs (sense and antisense of OVAAL) was mixed with extracted protein in RIP buffer (Thermo Fisher Scientific) for 1 h. After that, 50 μl streptavidin-linked beads (Invitrogen) were incubated with the RNA-protein binding reaction for 2 h at room temperature. The bead–RNA–protein complexes were diluted in SDS buffer. Finally, the retrieved proteins were measured using gradient gel electrophoresis followed by mass spectrometry analysis.

2.5 | RNA immunoprecipitation assay

RNA immunoprecipitation assays were carried out using the Magna RIP RNA-Binding Protein Immunoprecipitation Kit (Millipore) following the manufacturer's instructions. The retrieved RNAs were subjected to qRT-PCR analysis by using specific primers of sense OVAAL (Table S1). The IgG (Abcam) controls were assayed simultaneously to confirm that the RNA specifically interacted with PC.

2.6 | In vitro ubiquitination assay

Gastric cancer cells were treated with MG132 (10 μM; Selleck Chemicals) for 12h or 18h. Cell lysates were then collected and subjected to immunoprecipitation with anti-PC Ab (1:50 dilution); lysates were assessed by western blotting with anti-ubiquitin Ab (1:3000; Cell SignalingTechnology (CST)).

2.7 | Statistics

Statistical analysis was undertaken using SPSS version 22.0 (SPSS). Student's t-test was used for analysis of continuous variables and the χ^2-test or Fisher's exact test were applied to analyze categorical variables. Kaplan–Meier plots and log–rank tests were used for survival analyses. Univariable and multivariable Cox proportional hazards regression models were undertaken to analyze independent prognostic factors. The in vitro data are presented as mean ± SD for three independent experiments. All p values were two-sided. $p < 0.05$ was considered statistically significant

3 | RESULTS

3.1 | OVAAL is frequently upregulated in GC tissues and associated with poor outcome and 5-FU resistance

To identify the key lncRNAs that tightly linked to GC development, we first analyzed the differentially expressed lncRNAs in the TCGA GC dataset. From the 1541 upregulated and 437 downregulated lncRNAs between the tumor and normal tissues (Figure S1A,B), we screened out 151 prognosis-associated lncRNAs by Kaplan–Meier analysis and univariate Cox regression analysis (Figure 1A). To further narrow down to the most relevant lncRNAs in GC, we constructed a prognosis risk model using five lncRNAs (Figure 1B), considering higher HRs and smallest AIC. Survival analysis showed that the high risk score was significantly associated with the poor OS (Figure 1C) and higher mortality rate of GC patients (Figures 1D and S1C). The univariate and multivariate regression analyses also revealed that this risk model had the highest HR among the clinicopathologic characteristics and was an independent prognostic factor in the TCGA cohort (Table S2). The ROC curve showed that the 5-year value of area under the ROC was 0.739, indicating that our model was effective in GC progression prediction (Figure 1E)

Although each lncRNA in the model significantly correlated with the survival of TCGA GC patients, OVAAL showed the highest HR among them (Figures 1B,F,G and S1D–G). To further validate OVAAL expression in tissue samples, we undertook qRT-PCR in 34 pairs of GC tissues and matched nontumor tissues (cohort 1). Compared with nontumor tissues, OVAAL showed prominent increase in GC tissues (Figure 1H), which was consistent with the TCGA data (Figure 1I). Moreover, high level of OVAAL, detected by qRT-PCR in 120 GC tissues (cohort 2), was significantly associated with low OS and CSS (Figure 1J,K), larger tumor size, and lymph node metastasis (Table S3). The univariate and multivariate regression model also discovered that high OVAAL expression independently predicted poor OS and CSS in GC patients, with even higher HR than the local invasion (T stage) or distance metastasis (M stage) (Tables S4–S7)

5-Fluorouracil is widely applied in GC treatment as a basic chemotherapy drug. The sensitivity to 5-FU treatment markedly impacts the survival of GC patients. Interestingly, we discovered that the level of OVAAL was associated with the efficacy of 5-FU. Seventy-eight patients were treated with 5-FU-based adjuvant chemotherapy after surgery in cohort 2. High expression of OVAAL correlated with poor CSS in these patients (Figure 1L). These results suggested that a high OVAAL level was associated with tumor progression and efficacy of 5-FU treatment in GC.

3.2 | OVAAL promotes proliferation and increases resistance to 5-FU in GC cells

To functionally validate the above findings, we first tested the expression of OVAAL in four GC cell lines (AGS, BGC823, MGC803, and HGC-27) and normal gastric epithelial cells (GES-1), which showed relatively high levels of OVAAL in BGC823 and AGS lines (Figure S2A). We carried out subcellular fractionation assays in BGC823 and AGS lines, and found that OVAAL was mainly located in the cytoplasm (Figure S2B,C). Knocking down OVAAL by siRNA (Figure S2D,E) significantly impaired the proliferation of BGC823 and AGS cells, as detected by CCK-8 assays and colony formation
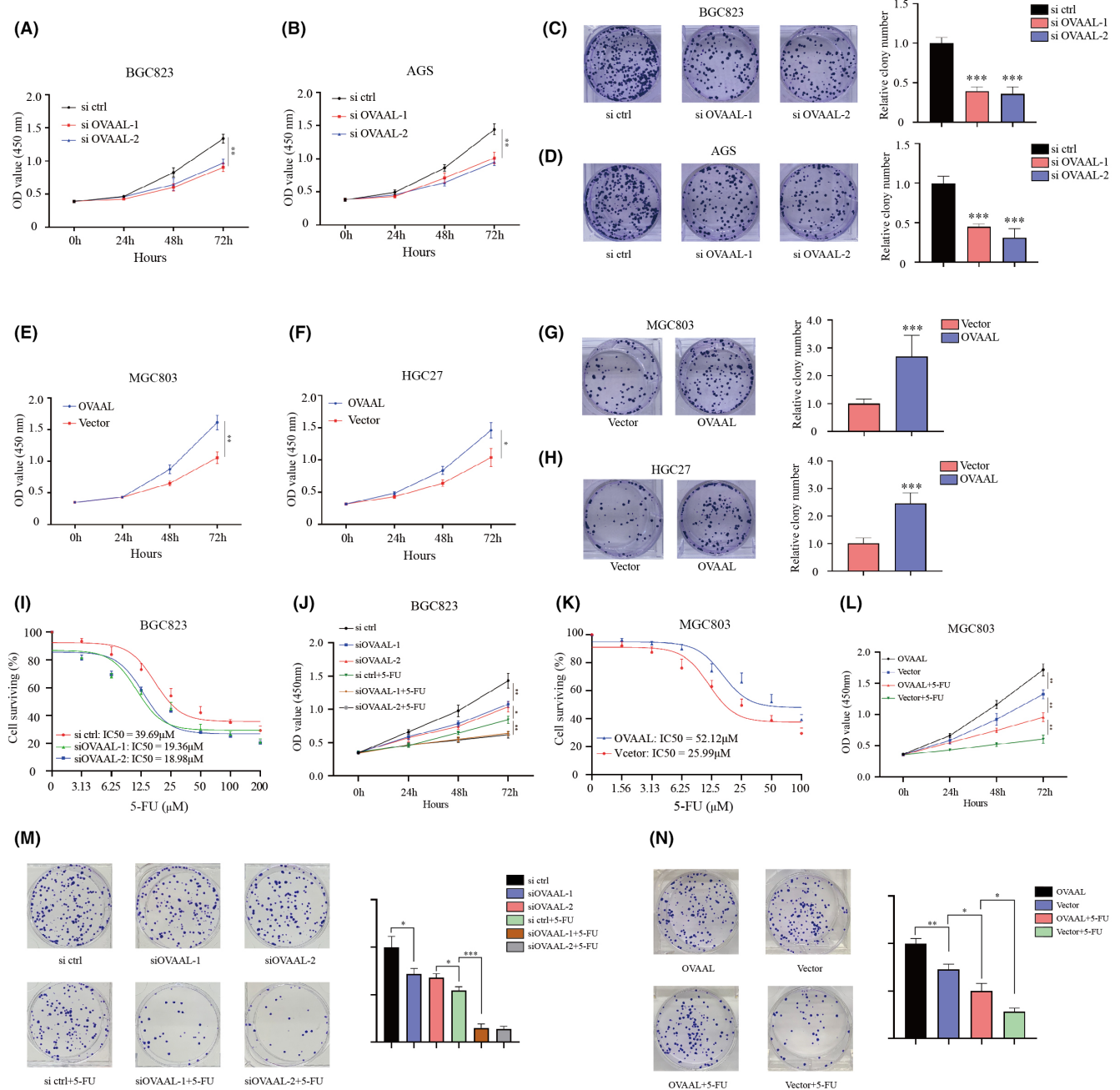
FIGURE 1 OVAAL is frequently upregulated in gastric cancer (GC) tissues and is associated with poor prognosis. (A) Spiral diagram illustrates the rank of lncRNAs associated with prognosis of GC patients. Red indicates the five long noncoding RNAs (lncRNAs) in the risk model. (B) Multivariate analysis of five lncRNAs in The Cancer Genome Atlas (TCGA) cohort. (C) Kaplan–Meier curve shows the overall survival (OS) of TCGA GC patients based on the risk score of five candidate lncRNAs. (D) Patient distribution of the risk score in the five-lncRNA panel. (E) Receiver operating characteristic (ROC) curve evaluates the diagnostic value of risk model in the TCGA cohort. Area under the ROC curve, 0.739. (F, G) Kaplan–Meier curve shows the OS and disease-free survival of TCGA GC patients. (H) Statistical analysis of OVAAL expression in 34 pairs of GC and normal tissues in cohort 1. ***$p < 0.001$, paired t-test. (I) Statistical analysis of OVAAL expression in GC and normal tissues in the TCGA dataset. *$p < 0.05$, unpaired t-test. (J, K) Survival analysis of GC patients in cohort 2, using the median expression of OVAAL as the cut-off value. (L) Kaplan–Meier curve shows the cancer-specific survival of GC patients treated with 5-fluorouracil (5-FU)-based chemotherapy in cohort 2. Median expression of OVAAL was used as the cut-off value. CI, confidence interval; HR, hazard ratio

assays (Figure 2A–D). Consistently, overexpressed OVAAL promoted MGC803 and HGC-27 cell proliferation in CCK-8 assays and colony formation assays (Figure 2E–H).

Furthermore, knockdown of OVAAL dramatically increased the sensitivity of BGC823 cells to 5-FU treatment, as shown by the reduced IC$_{50}$ values (Figure 2I), cell proliferation (Figure 2J),

FIGURE 2 OVAAL promotes proliferation and increases resistance to 5-fluorouracil (5-FU) in gastric cancer cells. (A–D) Cell proliferation colony formation assays using BGC823 and AGS cells transfected with OVAAL control (ctrl) or OVAAL siRNAs. (E–H) Cell proliferation and colony formation assays using MGC803 and HGC27 cells transfected with vector or OVAAL overexpression plasmid. (I) Dose–response curve shows relative 5-FU sensitivity of BGC823 cells. BGC823 cells were transfected with control or OVAAL siRNAs. (J) Cell proliferation assays using BGC823 cells transfected with control or OVAAL siRNAs and treated with 5-FU (30 μmol/L). (K) Dose–response curve shows relative 5-FU sensitivity of MGC803 cells. MGC803 cells were transfected with vector or OVAAL overexpression plasmid. (L) Cell proliferation assay using MGC803 cells transfected with vector or OVAAL overexpression plasmid and treated with 5-FU (30 μmol/L). (M) Colony formation assay using BGC823 cells transfected with control or OVAAL siRNAs and treated with 5-FU (30 μmol/L). (N) Colony formation assay using MGC803 cells transfected with vector or OVAAL overexpression plasmid and treated with 5-FU (30 μmol/L). Graphs represent mean ± SD of experimental triplicates. $^{*}p < 0.05$; $^{**}p < 0.01$; $^{***}p < 0.001$. OD, optical density

and colony formation (Figure 2M). Meanwhile, overexpression of OVAAL in MGC803 cells (Figure S2F,G) enhanced resistance to 5-FU, as assayed by IC$_{50}$ (Figure 2K), cell proliferation (Figure 2L),

and colony formation (Figure 2N). These results suggested that lncRNA OVAAL promoted GC cell proliferation and resistance to 5-FU treatment.

3.3 | OVAAL enhances pyrimidine nucleotide synthesis to promote proliferation and increase 5-FU resistance

5-Fluorouracil induces cancer cell death by impairing pyrimidine metabolism and DNA synthesis.[19] Growing evidence has suggested that lncRNAs promoted metabolism reprogramming to accelerate cancer progression.[20–22] Therefore, we tested whether lncRNA OVAAL induced 5-FU resistance of GC by regulating cancer cell metabolism, especially pyrimidine metabolism. Mass spectrometry analysis of the metabolite profiling showed that knockdown of OVAAL caused dramatic decrease of oxaloacetate in BGC823 cells (Figure 3A). Oxaloacetate is known to transform to citrate by condensing with acetyl CoA derived from a second pyruvate. Otherwise, oxaloacetate can undergo a transamination reaction to form aspartate. Consistent with the above knowledge, we observed the decrease of citrate (Figure 3A), as well as a significant decrease of aspartate among all amino acids (Figure 3B). However, glycolytic metabolites were not affected significantly following OVAAL knockdown (Figure S3A).

In cancer cells, de novo synthesis of nucleotides is the major source of nucleotide supplies.[23–25] Aspartate is essentially required for de novo synthesis of nucleotides (Figure S3B).[26] In purine biosynthesis, aspartate acts as nitrogen donor for the purine ring of inosine monophosphate, and the generated hypoxanthine is further converted into AMP or GMP.[27] More importantly, the whole structure of aspartate is used for pyrimidine ring synthesis, which is conjugated with carbamoyl phosphate to transform into carbamoyl aspartate and then converted into pyrimidine ring by dehydration and dehydrogenation. Thus, we hypothesized that the nucleotide synthesis, especially for pyrimidine nucleotide synthesis, would decrease following OVAAL knockdown because oxaloacetate and aspartate decreased following OVAAL knockdown. As expected, silencing OVAAL resulted in the reduction of the nucleosides pool in BGC823 cells, especially pyrimidine nucleosides UMP/UTP and CMP/CTP (Figure 3C). Moreover, silencing OVAAL reduced intracellular levels of dTMP (Figure 3D), which was in line with the report that dUMP could be transformed to dTMP by thymidylate synthase, therefore adding 5-FU would interfere with the dUMP to dTMP transformation, disturbing pyrimidine metabolism and inducing cancer cell death.[28] These results supported that OVAAL promoted NTPs, especially the pyrimidine nucleotide synthesis, to increase intracellular levels of dTMP, thus protecting GC from 5-FU-induced cell death.

To further confirm that OVAAL induced 5-FU resistance by enhancing pyrimidine metabolism, we directly replenished oxaloacetate, aspartate, or nucleotides to rescue the OVAAL-silencing phenotype. We found that repletion of oxaloacetate, aspartate, and uridine rescued the OVAAL silencing-induced decrease of 5-FU resistance (Figures 3E–J and S4A–F), whereas repletion of adenosine, guanosine, and cytidine could not (Figure S5A–C). These data supported that OVAAL could reprogram pyrimidine metabolism, therefore endowing GC cells with 5-FU resistance.

3.4 | OVAAL enhances pyrimidine metabolism and induces 5-FU resistance by interacting with pyruvate carboxylase

Next, we interrogated the mechanism of how OVAAL decreased the oxaloacetate levels and reprogrammed pyrimidine metabolism in GC. Like many other lncRNAs, we hypothesized that OVAAL might exert its function by interacting with proteins in the related pathway.[29] We undertook RNA pulldown assays in BGC-823 cells to identify the protein interacting with OVAAL. The proteins pulled down by the sense probe but not antisense probe were identified by mass spectrometry (Figure 4A). Pyruvate carboxylase was the top scored protein identified by mass spectrometry (Figure 4B). The binding of OVAAL with PC was verified by western blot analysis following the RNA pull-down assay (Figure 4C). In line with these results, the RIP assays showed the interaction between OVAAL and PC in BGC823 and AGS cells (Figure 4D). Pyruvate carboxylase catalyzes the carboxylation of pyruvate to oxaloacetate, which acts as the precursor for the synthesis of many C4 intermediates in TCA and other metabolic programs.[30] Dysfunction of PC would block the transition of pyruvate to oxaloacetate, which was consistent with our observation that knocking down OVAAL resulted in the decrease of oxaloacetate and the subsequent metabolites, including citrate and aspartate. Thus, we hypothesized that OVAAL enhanced the oxaloacetate production and the subsequent pyrimidine metabolism by activating PC.

Then we tested whether PC mediated the biological function of OVAAL in GC. We transfected PC into OVAAL-silenced BGC823 cells. Mass spectrometry analysis showed that exogenous expression of PC could rescue the decreased oxaloacetate, citrate, and aspartate in OVAAL-silencing BGC823 cells (Figure 4E–G), as well as NTPs and dTMP (Figure 4H,I). In line with the results, overexpression

FIGURE 3 Long noncoding RNA (lncRNA) OVAAL promotes proliferation and increases resistance to 5-fluorouracil (5-FU) by regulating nucleotide metabolism. (A–C) Liquid chromatography–mass spectrometry (LC–MS) analysis showed that knocking down OVAAL impaired the intracellular level of tricarboxylic acid cycle metabolites, amino acids, and nucleotides. (D) LC–MS analysis showed that knocking down OVAAL impaired the intracellular level of dTMP. (E) The 5-FU dose–response curve shows the effect of oxaloacetate (8 mM) repletion on OVAAL-silenced BGC823 cells. (F) Oxaloacetate (8 mM) repletion rescues OVAAL knockdown-induced decrease of cell viability under 5-FU treatment (30 μmol/L). (G) The 5-FU dose–response curve shows the effect of aspartate (6 mM) repletion on OVAAL-silenced BGC823 cells. (H) Aspartate (6 mM) repletion rescues OVAAL knockdown-induced decrease of cell viability under 5-FU treatment (30 μmol/L). (I) The 5-FU dose–response curve shows the effect of uridine (100 μM) repletion on OVAAL-silenced BGC823 cells. (J) Uridine (100 μM) repletion rescues OVAAL knockdown-induced decrease of cell viability under 5-FU treatment (30 μmol/L). Graphs represent mean ± SD of experimental triplicates. *$p < 0.05$; **$p < 0.01$; ***$p < 0.001$. OD, optical density
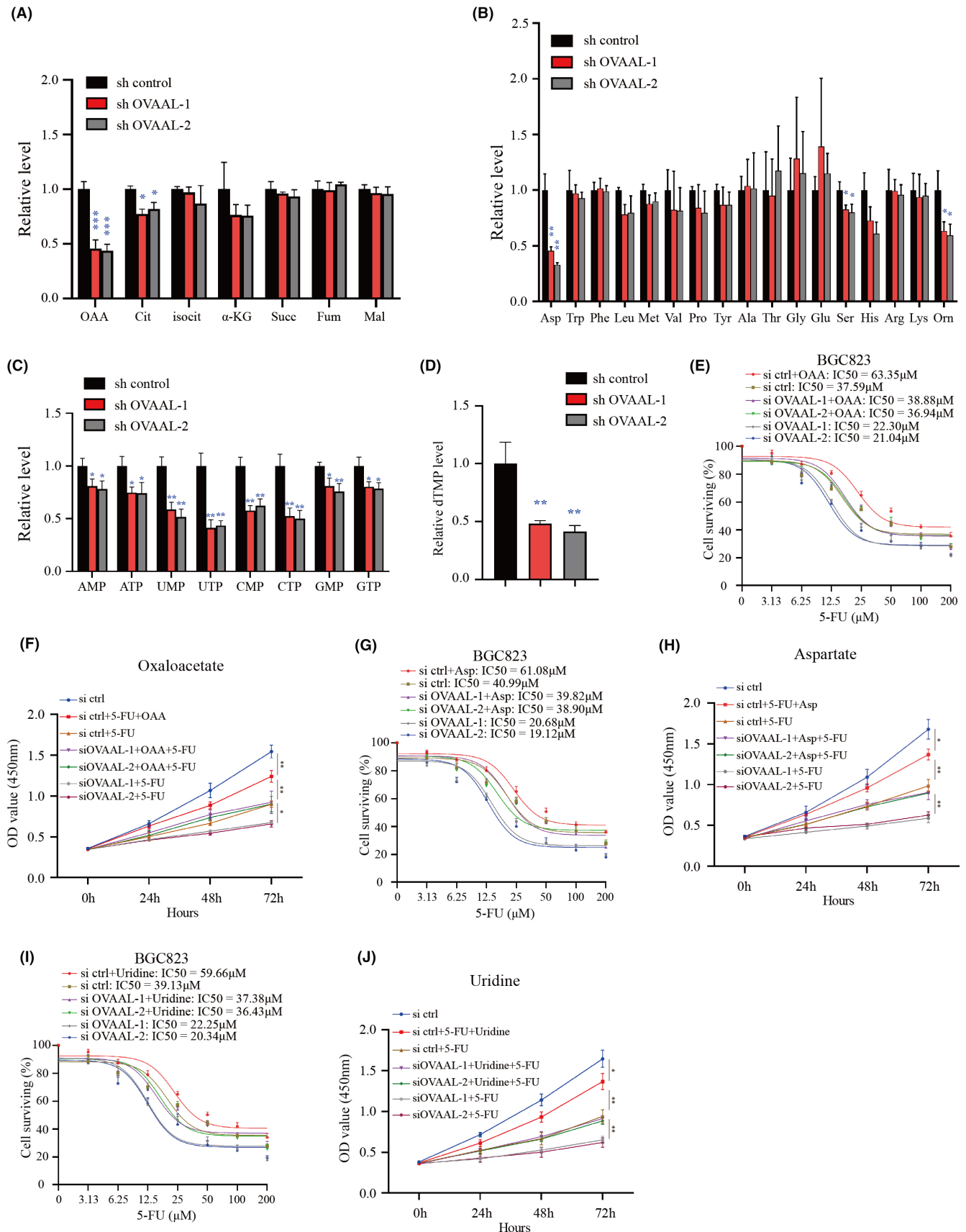
of PC could significantly rescue the OVAAL silencing-induced reduction of 5-FU resistance, as measured by IC_{50} values and the cell proliferation assay (Figures 4J,K and S6A). Likewise, we transfected

PC siRNAs into OVAAL-overexpressing MG803 cells. Pyruvate carboxylase knockdown could reduce the increased level of oxaloacetate, citrate, aspartate, NTPs, and dTMP in OVAAL-overexpressing
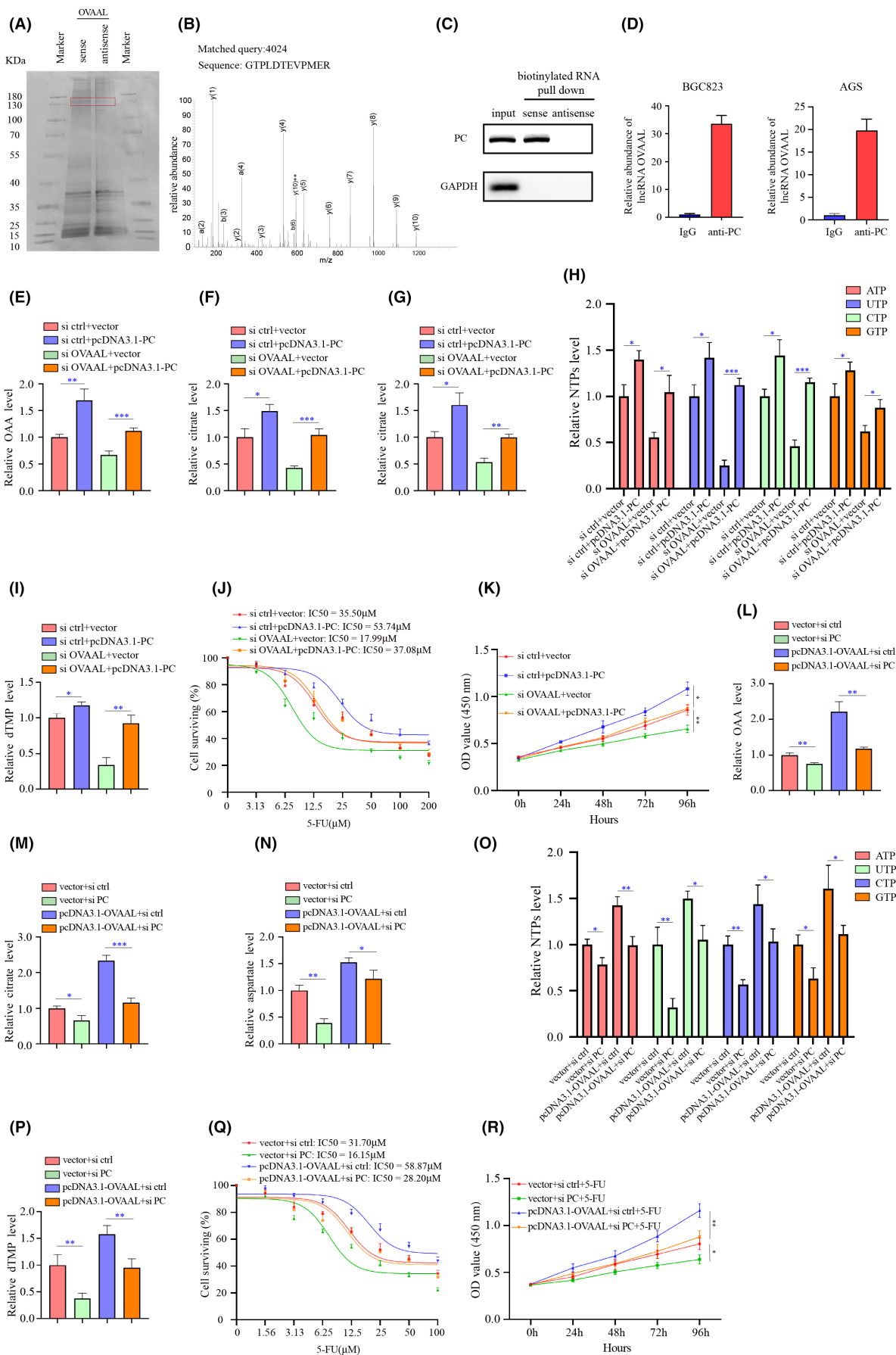
FIGURE 4 OVAAL enhances pyrimidine nucleotide synthesis by interacting with pyruvate carboxylase (PC) to promote proliferation and increase 5-fluorouracil (5-FU) resistance. (A) Silver-stained SDS-PAGE gel of proteins pulled down by OVAAL or its control antisense RNA in BGC823 cells. Framed bands were identified by mass spectrometry. (B) PC was identified by mass spectrometry. (C) RNA pull-down followed by western blot showed the binding of OVAAL to PC. (D) RNA immunoprecipitation assays using PC Ab followed by quantitative RT-PCR showed the binding of OVAAL to PC in BGC823 and AGS cells. (E–G) Decreased intracellular concentration of oxaloacetate, citrate, and aspartate in OVAAL knockdown BCG823 cells was restored by PC overexpression. (H, I) Decreased intracellular concentrations of nucleotide triphosphate (NTP) and deoxythymidine monophosphate (dTMP) in OVAAL knockdown BCG823 cells were restored by PC overexpression. (J) The dose–response curve showed that increased 5-FU sensitivity in OVAAL-silenced BGC823 cells was abolished by PC overexpression. (K) Decreased cell viability in OVAAL-silenced BGC823 cells was restored by PC overexpression. BGC cells were treated with 5-FU (30 μmol/L). (L–N) Increased intracellular concentrations of oxaloacetate, citrate, and aspartate in OVAAL-overexpression MGC803 cells were abolished by PC knockdown. (O, P) Increased intracellular concentrations of NTPs and dTMP in OVAAL-overexpressing MGC803 cells were abolished by PC knockdown. (Q) The dose–response curve showed that decreased 5-FU sensitivity in OVAAL-overexpression MGC803 cells was restored by PC knockdown. (R) Increased cell viability in OVAAL-overexpressing MGC803 cells was abolished by PC knockdown. MGC803 cells were treated with 5-FU (30 μmol/L). All data are presented as mean ± SD of experimental triplicates. *$p < 0.05$; **$p < 0.01$; ***$p < 0.001$. ATP, adenosine triphosphate; CTP, cytidine triphosphate; ctrl, control; GTP, guanosine triphosphate; lncRNA, long noncoding RNA; OAA, Oxaloacetate; OD, optical density; UTP, uridine triphosphate

MGC803 cells (Figure 4L–P). Consistently, PC siRNAs significantly abrogated OVAAL overexpression-induced 5-FU resistance (Figures 4Q,R and S6B). These data together indicated that OVAAL regulated nucleotide metabolism and 5-FU resistance through PC in GC.

3.5 | OVAAL promotes pyruvate carboxylase activity by increasing its stability

To identify which region of OVAAL interacted with PC, we constructed five fragments of OVAAL (F1, full length of OVAAL; F2, 1–500 nt; F3, 501–1000 nt; F4, 1001–1489 nt; F5, 1–750 nt; and F6, 751–1489 nt). The RNA pull-down assay using these fragments as probes showed that F3 and F6 could physically bind to PC (Figure 5A), which suggested that 751–1000 nt was the region in OVAAL that interacted with PC.

We further constructed the specific fragment (Fs, 751–1000 nt) of OVAAL and the mutant lacking the Fs fragment (ΔFs). The functional assays and western blot analysis showed that overexpression of Fs, but not ΔFs, was sufficient to rescue the IC$_{50}$ of 5-FU (Figure 5B,C) and the protein level of PC after OVAAL knockdown (Figure 5D). These data together suggested fragment 751–1000 nt was crucial for the function of OVAAL.

Next, we explored how OVAAL regulated PC function. We detected a significant decrease of the PC protein level following OVAAL silencing in BGC-823 cells and an increase of the PC protein level in MGC-803 cells overexpressing OVAAL (Figure 5E,F). However, the mRNA levels of PC were not affected upon OVAAL RNAi or exogenous expression (Figure S7A,B), suggesting that OVAAL increased the levels of PC protein at the post-transcriptional level. We then tested whether OVAAL influenced PC protein degradation. BGC823 cells were treated with the protein synthesis inhibitor cycloheximide, which showed an accelerated degradation of PC protein after OVAAL knockdown (Figure 5G,H). To rule out the possibility that OVAAL might regulate the PC protein synthesis, we treated BGC823 cells with the proteasome inhibitor MG-132,

and found OVAAL silencing-induced PC protein downregulation was abolished (Figure 5I). These results supported that OVAAL increased the PC level by regulating its proteasome-dependent degradation, but not synthesis. We further confirmed these results by the ubiquitination assay, which showed that knocking down OVAAL increased the level of PC ubiquitination in BGC823 cells (Figure 5J). Consistently, overexpressed OVAAL decreased the level of PC ubiquitination (Figure 5K). These results illustrated that OVAAL interacted with PC and prevented the ubiquitin-mediated degradation of PC protein.

In order to explore the underlying mechanism of how OVAAL protects PC from protein degradation, we used UbiBrowser 2.0 (http://ubibrowser.ncpsb.org.cn) to predict the potential E3 ligase of PC.[31] UbiBrowser 2.0 predicted that HSC70 was the potential protein that interacted with PC to induce ubiquitin degradation. To validate the prediction, we used the Co-IP assay followed by mass spectrometry to compare PC binding proteins in control and OVAAL knockdown cells (Figure 6A). In PC-immunoprecipitated complexes, HSC70 was detected in OVAAL knockdown BGC-823 cells by mass spectrum (Figure 6B), but not in control cells, indicating that OVAAL weakened the interaction between PC and HSC70. The Co-IP experiment also confirmed the interaction between PC and HSC70 in BGC823 cells (Figure 6C). In addition, knockdown of OVAAL strengthened the interaction between PC and HSC70 (Figure 6D), without influencing the protein level of HSC70 (Figure S8A). Moreover, knockdown of HSC70 significantly decreased PC ubiquitination (Figure 6E) and increased PC protein levels (Figure 6F,G). HSC70 may function as molecular chaperon and CHIP is an important E3 ligase, which forms the HSC70/CHIP complex to modify substrate targeting and facilitate protein degradation.[32,33] As expected, the Co-IP assay validated the interaction between HSC70 and CHIP in BGC823 cells (Figure 6H). Knockdown of OVAAL did not influence the protein level of CHIP (Figure S8B). However, knockdown of CHIP could significantly decrease the ubiquitination of PC (Figure 6I) and upregulate the protein level of PC (Figure 6J). These data indicated that OVAAL prevented the interaction between PC and HSC70, thereby further blocking the ubiquitination and degradation of PC by CHIP.
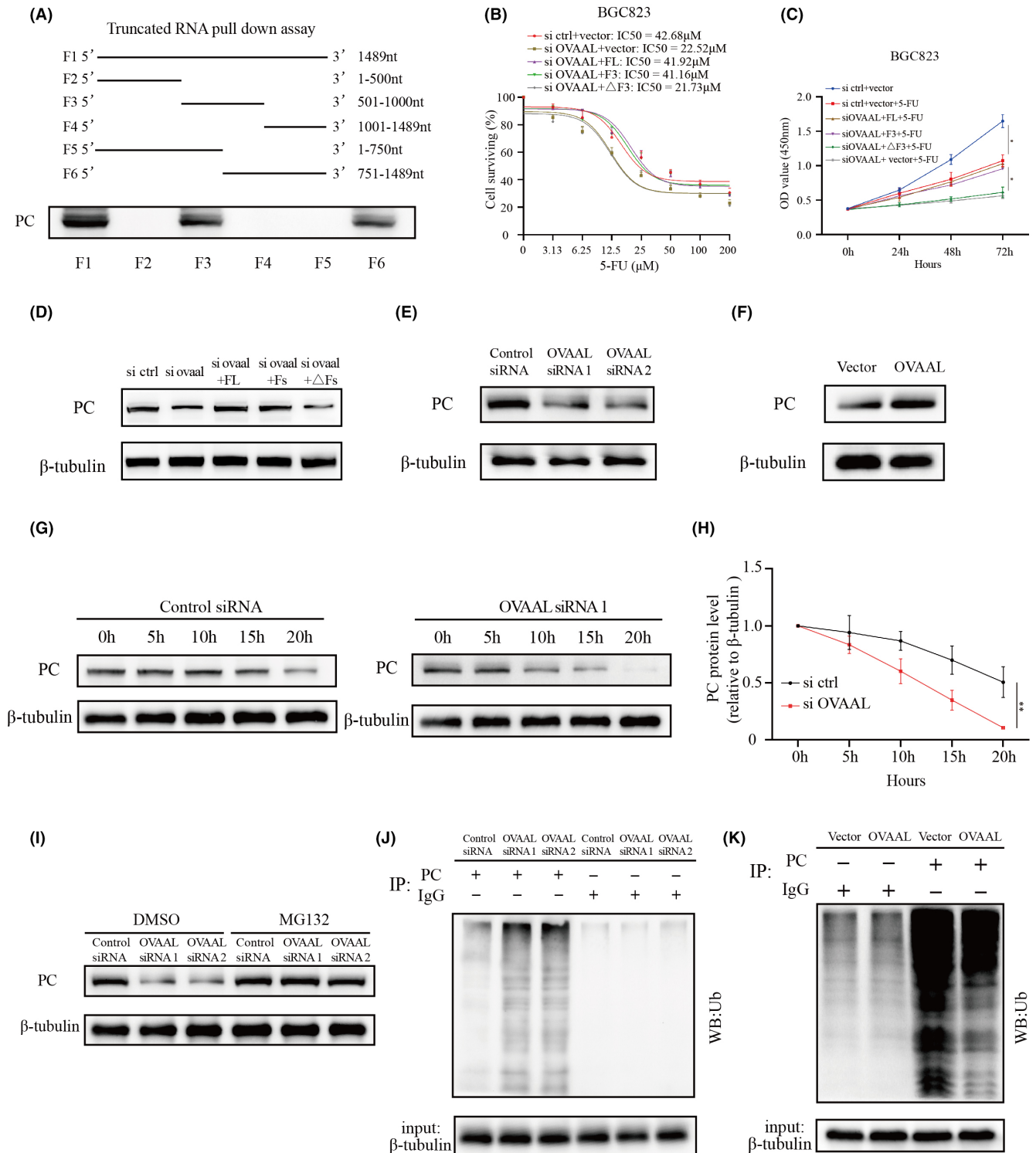
FIGURE 5 OVAAL enhances pyruvate carboxylase protein level by increasing its stability. (A) Full-length (F1) or truncated long noncoding RNA (lncRNA) OVAAL (F2, 1–500 nt; F3, 501–1000 nt; F4, 1001–1489 nt; F5,1–750 nt; F6,751–1489 nt) were used to pull down proteins. (B) The dose–response curve showed that increased 5-fluorouracil (5-FU) sensitivity in OVAAL-silenced BGC823 cells was abolished by Fs (751-1000 nt) fragment overexpression. (C) Decreased cell viability in OVAAL-silenced BGC823 cells was restored by Fs overexpression. BGC cells were treated with 5-FU (30 μmol/L). (D) Western blot detected protein levels of pyruvate carboxylase (PC) in Full-length (FL), Fs or ΔFs (mutant lacking the Fs fragment) transfected BGC823 cells treated with OVAAL siRNA. (E) Western blot detected protein levels of PC in OVAAL-silenced BGC823 cells with its control. (F) Western blot detected protein levels of PC in OVAAL-overexpressing MGC823 cells with its control. (G, H) Cycloheximide chase assay of PC in OVAAL stable knockdown BGC823 cells. (I) Western blot analysis detected the protein levels of PC in OVAAL-silenced BCG823 cells and its control. BGC823 cells were treated with MG132 (10 μmol/L) for 18 h. (J) OVAAL knockdown promotes the ubiquitination of PC. BGC823 cells were treated with MG132 (10 μmol/L) for 18 h. (K) OVAAL overexpression reduces the ubiquitination of PC. MGC803 cells were treated with MG132 (10 μmol/L) for 12 h. ctrl, control
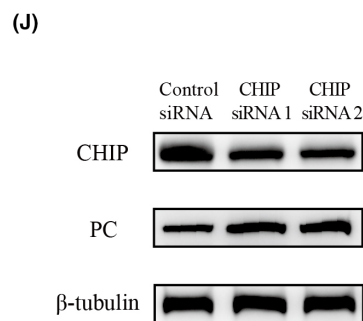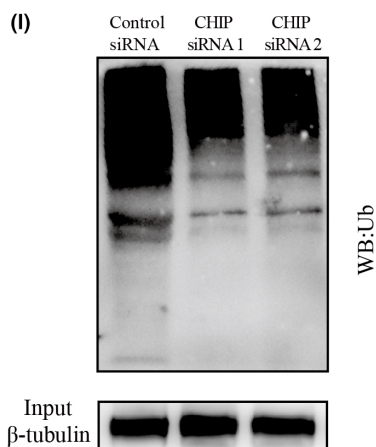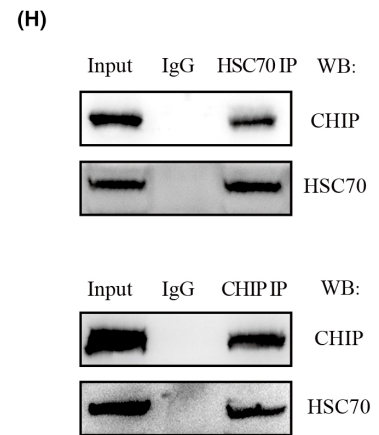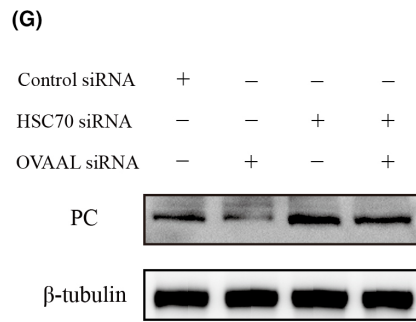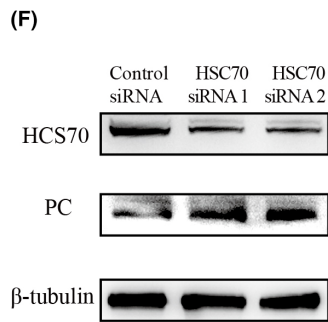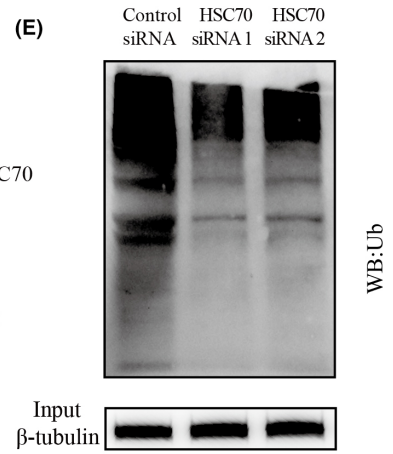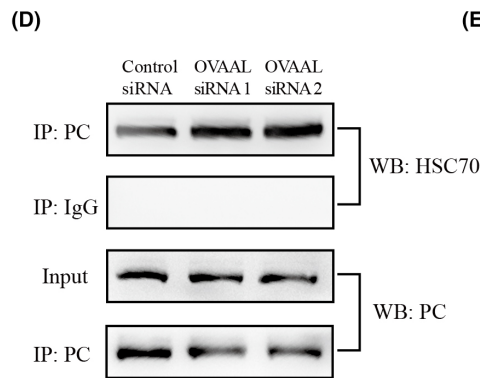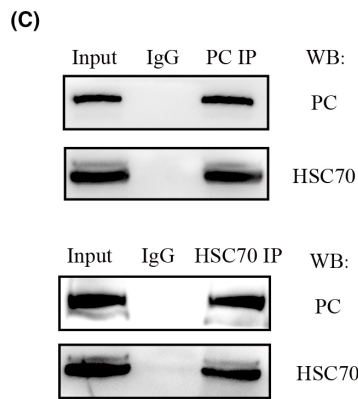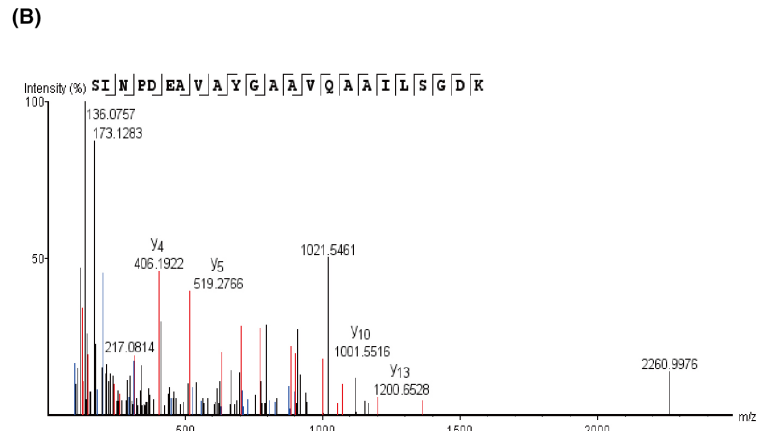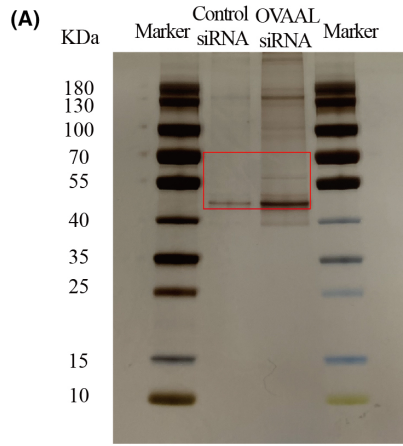
FIGURE 6 (Continued)

FIGURE 6 OVAAL prevents the interaction between pyruvate carboxylase (PC) and HSC70 to block the ubiquitination and degradation of PC by CHIP. (A) Silver-stained SDS-PAGE gel of proteins immunoprecipitated (IP) by PC Ab in control and OVAAL knockdown BGC823 cells. Framed bands were identified by mass spectrometry. (B) HSC70 identification by mass spectrometry. (C) Co-immunoprecipitation (Co-IP) detected interaction between PC and HSC70 in the BGC823 cells. (D) Co-IP detected interaction between PC and HSC70 in OVAAL-silenced BGC823 cells with its control. (E) HSC70 knockdown reduced the ubiquitination (Ub) of PC. BGC823 cells were treated with MG132 (10 μmol/L) for 18 h. (F) Western blot (WB) detected protein levels of PC in HSC70-silenced BGC823 cells with its control. (G) WB detected protein levels of PC after HSC70 knockdown in OVAAL-silenced BCG823 cells and its control. (H) Co-IP detected interaction between HSC70 and CHIP in BGC823 cells. (I) CHIP knockdown reduced the ubiquitination of PC. BGC823 cells were treated with MG132 (10 μmol/L) for 18 h. (J) WB detected protein levels of PC in CHIP-silenced BGC823 cells with its control

3.6 | Targeting OVAAL decreases resistance of 5-FU in GC xenografts

To examine the role of OVAAL in chemoresistance in vivo, we injected control shRNA or OVAAL shRNA-expressing BGC823 cells into the right dorsal flank of 4-week-old male BALB/C nude mice and treated with 5-FU (15 mg/kg) or PBS every 3 days. OVAAL knockdown slightly decreased the growth of BGC823 xenografts in nude mice (Figures 7A–C and S9). Chemotherapy with 5-FU moderately lowered the tumor growth. However, OVAAL knockdown synergized with 5-FU therapy almost completely inhibited tumor growth (Figures 7A–C and S9A). In line with these observations, the percentage of Ki-67-positive cells decreased moderately in OVAAL knockdown tumors and 5-FU treated tumors, whereas Ki-67 staining was almost negative in tumors treated by the OVAAL knockdown and 5-FU combination (Figure 7D,E). In addition, the expression of PC also decreased along with the OVAAL knockdown in tumors (Figure 7F,G).

To further explore whether OVAAL exerted its role in chemoresistance through PC, we injected vector or pcDNA3.1 PC in OVAAL shRNA-expressing BGC823 cells into the right dorsal flank of BALB/C nude mice and treated with 5-FU (15 mg/kg) or PBS every 3 days (Figure S10). Overexpression of PC promoted tumor growth of BGC823 xenografts in nude mice with or without 5-FU treatment (Figure 7H–J). Consistently, the percentage of Ki-67-positive cells in vector groups was weaker than in pcDNA3.1 PC groups (Figures 7K–N and S9B).

Together, these results suggested that knockdown of OVAAL might be a promising strategy to overcome resistance of 5-FU as well as to prevent GC progression (Figure 8).

4 | DISCUSSION

5-Fluorouracil has been widely applied in chemotherapy of GC for decades.[34,35] However, 5-FU-based chemotherapy, as first-line treatment, has shown limited response rates; the objective responses of the single agent tended to be <20%,[36] and 5-FU-based doublets (cisplatin/5-FU) or triplets (cisplatin/epirubicin/5-FU) typically reached a response rate of up to 50%.[37] It is urgent to find new therapeutic strategies to overcome 5-FU resistance. Herein, we identified a crucial lncRNA OVAAL that was associated with poor prognosis of GC patients and patients with 5-FU-based adjuvant chemotherapy. In vitro and in vivo assays confirmed that OVAAL promoted GC cell proliferation and 5-FU resistance. OVAAL has been reported to confer apoptotic resistance to melanoma and colorectal cancer by activating the RAF/MEK/ERK signaling cascade,[38] but the mechanism of OVAAL in 5-FU resistance of GCs is different.

5-Fluorouracil is a pyrimidine analogue working as an antimetabolite to disturb the pyrimidine metabolism of cancers, thus leading to cancer cell death. Apparently, recovering the pyrimidine metabolism would be a direct way to overcome the 5-FU-induced cancer cell death. Metabolic screening revealed that knocking down OVAAL decreased the levels of oxaloacetate. Oxaloacetate and α-ketoglutarate are the major intermediates that fuel TCA. In addition, oxaloacetate can be transaminated to form aspartate by aspartate transaminase.[39] In starvation, oxaloacetate can be converted to phosphoenolpyruvate for gluconeogenesis.[40] Adding 5-FU can interfere with thymidylate synthase-catalyzed dUTP to dTMP transformation, which then disrupts DNA synthesis and repair in cancer cells.[41,42] Thus, the pyrimidine metabolism is disturbed following 5-FU treatment. To survive under this stress, cancer cells have to

FIGURE 7 Targeting OVAAL decreases resistance of 5-fluorouracil (5-FU) in gastric cancer xenografts. (A–C) Tumor image (A), growth curves (B), and tumor weights (C) of BGC823 xenografts. BGC823 cells transfected with control or OVAAL shRNAs were subcutaneously inoculated into nude mice. 5-FU was injected intraperitoneally into mice (15 mg/kg every 3 days). (D, E) Representative immunohistochemistry (IHC) images (D) and staining scores (E) of Ki-67 in paraffin-embedded xenograft sections (magnification, ×400). (F, G) Representative IHC images (F) and staining scores (G) of pyruvate carboxylase (PC) in paraffin-embedded xenograft sections (magnification, ×400). (H–J) Tumor image (H), growth curves (I), and tumor weights (J) of BGC823 xenografts. Sh-OVAAL BGC823 cells transfected with vector or pcDNA3.1-PC were subcutaneously inoculated into nude mice. 5-FU was injected intraperitoneally in mice (15 mg/kg every 3 days). (K, L) Representative IHC images (K) and staining scores (L) of Ki-67 in paraffin-embedded xenograft sections (magnification, ×400). (M, N) Representative IHC images (M) and staining scores (N) of PC in paraffin-embedded xenograft sections (magnification, ×400). Data of tumor volume, weight, and IHC score are mean ± SD of six mice in each group. **$p < 0.01$; ***$p < 0.001$
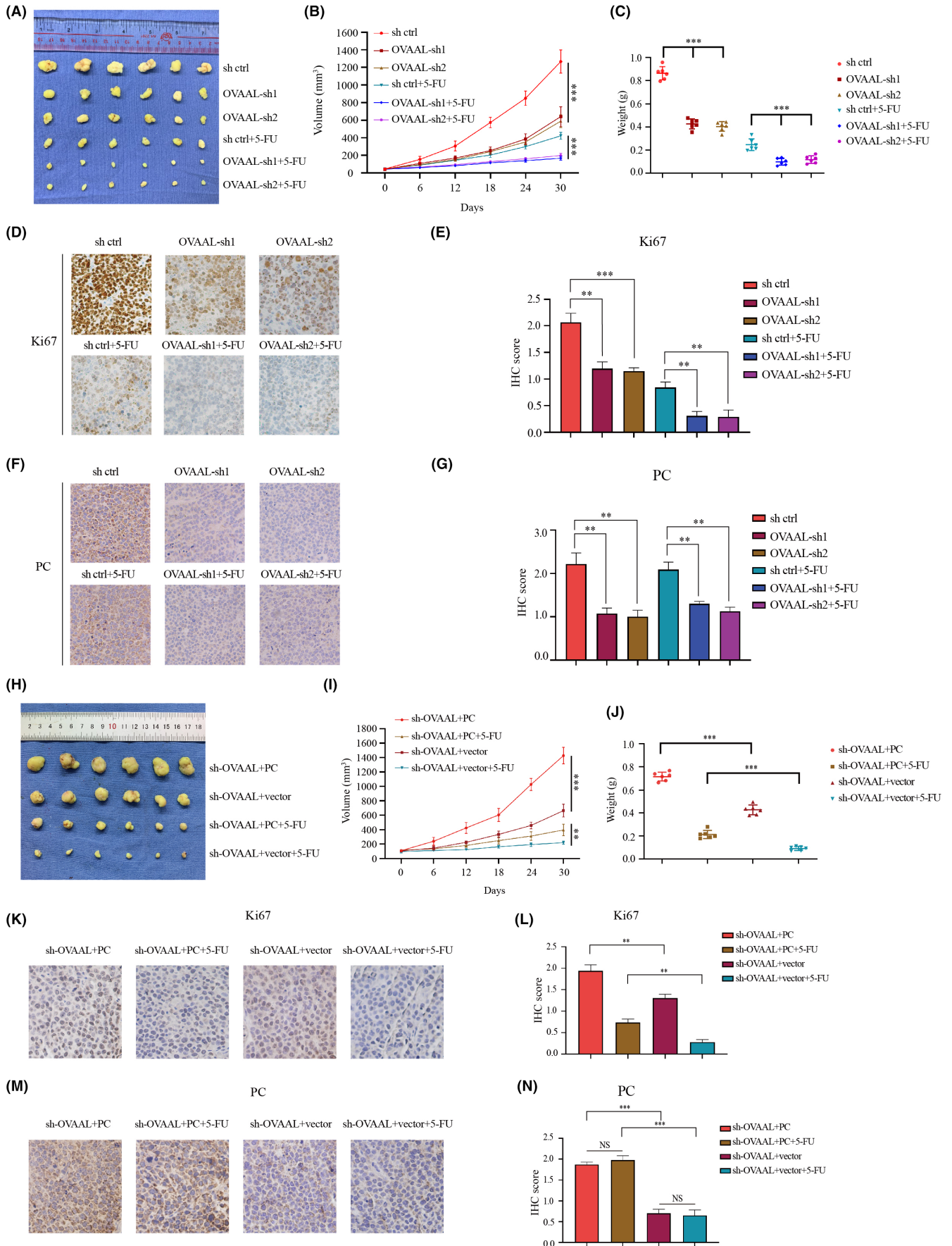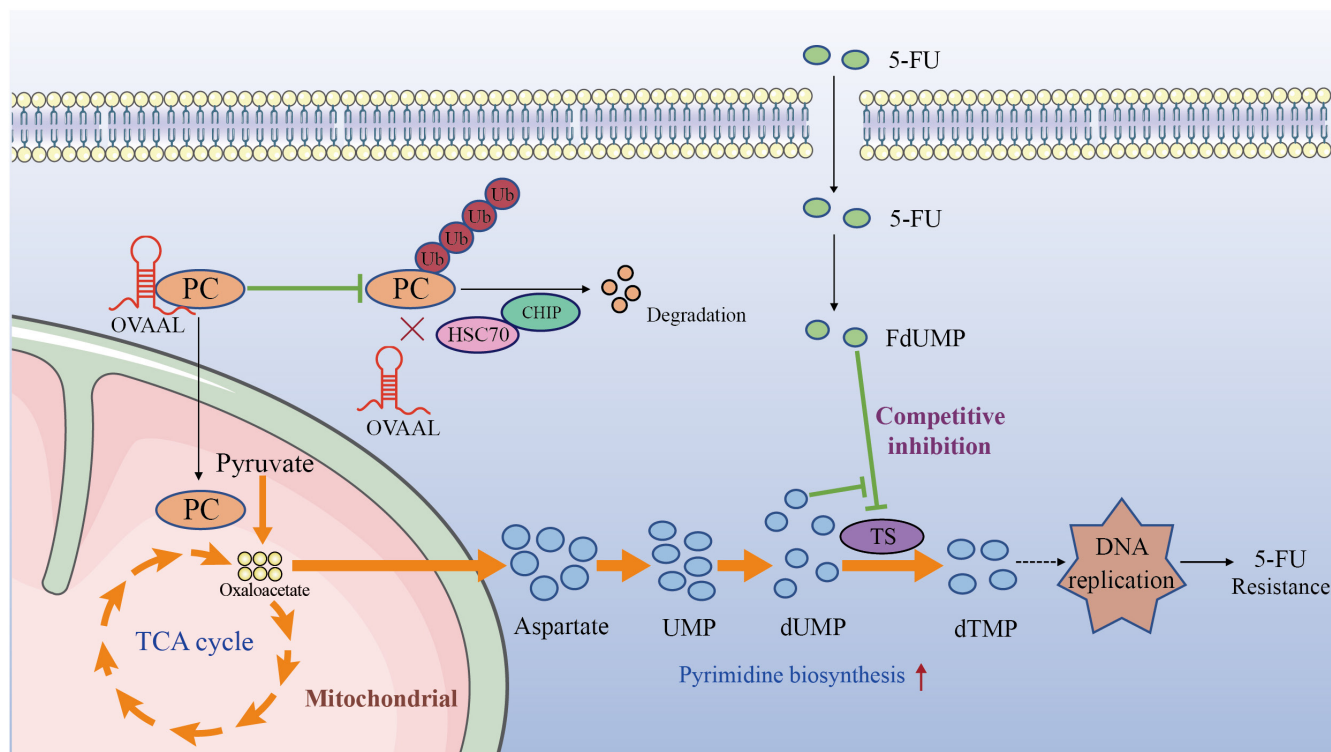
FIGURE 8 Graphic illustration of the mechanism through which OVAAL increases resistance of 5-fluorouracil (5-FU) by stabilizing pyruvate carboxylase (PC) in gastric cancer cells. OVAAL blocks the interaction between PC and HSC70/CHIP and stabilizes PC, which results in enhanced production of oxaloacetate and aspartate, and promotes nucleotide biosynthesis, therefore protecting gastric cancer cells from 5-FU treatment and providing sufficient nucleotides to support DNA replication and repair. dTMP, deoxythymidine monophosphate; dUMP, deoxyuridine monophosphate; FdUMP, fluorodeoxyuridine diphosphate; TCA, tricarboxylic acid cycle; TS, thymidylate synthase; Ub, ubiquitination; UMP, uridine monophosphate

overcome the disorder. Additional pyrimidine supply would be a direct rescue to the pyrimidine metabolism disorder. Overexpression of OVAAL results in less proteasomal degradation of PC, which leads to the accumulation of PC and accelerated production of oxaloacetate from pyruvate. Subsequently, aspartate production and the following pyrimidine metabolism are enhanced, which helps cancer cells to overcome the 5-FU induced pyrimidine metabolic abnormalities. Consistently, repletion of oxaloacetate, aspartate, and uridine, but not adenosine/guanosine/cytidine, reverses the proliferation suppression and increased sensitivity to 5-FU treatment induced by OVAAL knockdown.

In summary, our data revealed that lncRNA OVAAL stabilized pyruvate carboxylase and accelerated oxaloacetate-aspartate production and thus enhanced pyrimidine biosynthesis, which promoted GC cell proliferation and the resistance to 5-FU. Our finding also indicated that the level of OVAAL could serve as potential biomarker for 5-FU resistance and poor outcome of GCs. More importantly, our study provided a potential therapeutic strategy of preventing GC progression and overcoming 5-FU resistance by targeting OVAAL and pyrimidine metabolism.

AUTHOR CONTRIBUTIONS

JNT, SNZ, and WZ were responsible for performing experiments, acquisition of data, and writing the manuscript. BY and GYZ collected the clinical samples and clinical data. JH checked and analyzed the data. HH provided technical support. FHH and MLL were responsible for designing the experiments, manuscript writing and revision. The authors read and approved the final manuscript.

DISCLOSURE

The authors have no conflict of interest.

DATA AVAILABILITY STATEMENT

The datasets used or analyzed during the current study are available from the corresponding author on reasonable request.

ETHICS STATEMENT

This research was approved by the Ethics Committee of Sun Yat-Sen Memorial Hospital. All tissues samples were obtained with informed consent from Sun Yat-Sen Memorial Hospital. The mice were raised

in the Laboratory Animal Center of Sun Yat-Sen University and the animal experiments were performed according to the animal ethical guidelines.

ORCID

Man-Li Luo https://orcid.org/0000-0002-6435-7303

REFERENCES

1. Bray F, Ferlay J, Soerjomataram I, Siegel RL, Torre LA, Jemal A. Global cancer statistics 2018: GLOBOCAN estimates of incidence and mortality worldwide for 36 cancers in 185 countries. *CA Cancer J Clin.* 2018;68:394-424.
2. Thrift AP, El-Serag HB. Burden of gastric cancer. *Clin Gastroenterol Hepatol.* 2020;18:534-542.
3. Biagioni A, Skalamera I, Peri S, et al. Update on gastric cancer treatments and gene therapies. *Cancer Metastasis Rev.* 2019;38:537-548.
4. Sun TT, He J, Liang Q, et al. LncRNA GClnc1 promotes gastric carcinogenesis and may act as a modular scaffold of WDR5 and KAT2A complexes to specify the histone modification pattern. *Cancer Discov.* 2016;6:784-801.
5. Zhuo W, Liu Y, Li S, et al. Long noncoding RNA GMAN, up-regulated in gastric cancer tissues, is associated with metastasis in patients and promotes translation of ephrin A1 by competitively binding GMAN-AS. *Gastroenterology.* 2019;156:676-691.e611.
6. Yang Q, Li K, Huang X, et al. lncRNA SLC7A11-AS1 promotes chemoresistance by blocking SCF(β-TRCP)-mediated degradation of NRF2 in pancreatic cancer. *Mol Ther Nucleic Acids.* 2020;19:974-985.
7. Huarte M. The emerging role of lncRNAs in cancer. *Nat Med.* 2015;21:1253-1261.
8. Kogo R, Shimamura T, Mimori K, et al. Long noncoding RNA HOTAIR regulates polycomb-dependent chromatin modification and is associated with poor prognosis in colorectal cancers. *Cancer Res.* 2011;71:6320-6326.
9. Gutschner T, Hämmerle M, Eissmann M, et al. The noncoding RNA MALAT1 is a critical regulator of the metastasis phenotype of lung cancer cells. *Cancer Res.* 2013;73:1180-1189.
10. Shi X, Sun M, Liu H, et al. A critical role for the long non-coding RNA GAS5 in proliferation and apoptosis in non-small-cell lung cancer. *Mol Carcinog.* 2015;54(Suppl 1):E1-E12.
11. Wang Z, Wang Q, Xu G, et al. The long noncoding RNA CRAL reverses cisplatin resistance via the miR-505/CYLD/AKT axis in human gastric cancer cells. *RNA Biol.* 2020;17:1576-1589.
12. Lin X, Dinglin X, Cao S, et al. Enhancer-driven lncRNA BDNF-AS induces endocrine resistance and malignant progression of breast cancer through the RNH1/TRIM21/mTOR cascade. *Cell Rep.* 2020;31:107753.
13. Warburg O. On the origin of cancer cells. *Science (New York, NY).* 1956;123:309-314.
14. Zheng F, Chen J, Zhang X, et al. The HIF-1α antisense long noncoding RNA drives a positive feedback loop of HIF-1α mediated transactivation and glycolysis. *Nat Commun.* 2021;12:1341.
15. Chen F, Chen J, Yang L, et al. Extracellular vesicle-packaged HIF-1α-stabilizing lncRNA from tumour-associated macrophages regulates aerobic glycolysis of breast cancer cells. *Nat Cell Biol.* 2019;21:498-510.
16. Li Q, Qin T, Bi Z, et al. Rac1 activates non-oxidative pentose phosphate pathway to induce chemoresistance of breast cancer. *Nat Commun.* 2020;11:1456.
17. Wang T, Fahrmann JF, Lee H, et al. JAK/STAT3-regulated fatty acid β-oxidation is critical for breast cancer stem cell self-renewal and chemoresistance. *Cell Metab.* 2018;27:136-150.e135.
18. Blomme A, Ford CA, Mui E, et al. 2,4-dienoyl-CoA reductase regulates lipid homeostasis in treatment-resistant prostate cancer. *Nat Commun.* 2020;11:2508.

19. Xie P, Mo JL, Liu JH, et al. Pharmacogenomics of 5-fluorouracil in colorectal cancer: review and update. *Cell Oncol (Dordr).* 2020;43:989-1001.
20. Wang Y, Lu JH, Wu QN, et al. LncRNA LINRIS stabilizes IGF2BP2 and promotes the aerobic glycolysis in colorectal cancer. *Mol Cancer.* 2019;18:174.
21. Zheng X, Han H, Liu GP, et al. LncRNA wires up Hippo and Hedgehog signaling to reprogramme glucose metabolism. *EMBO J.* 2017;36:3325-3335.
22. Wang C, Li Y, Yan S, et al. Interactome analysis reveals that lncRNA HULC promotes aerobic glycolysis through LDHA and PKM2. *Nat Commun.* 2020;11:3162.
23. Villa E, Ali ES, Sahu U, Ben-Sahra I. Cancer Cells Tune the Signaling Pathways to Empower de Novo Synthesis of Nucleotides. *Cancer.* 2019;11:688.
24. Tong X, Zhao F, Thompson CB. The molecular determinants of de novo nucleotide biosynthesis in cancer cells. *Curr Opin Genet Dev.* 2009;19:32-37.
25. Vander Heiden MG, DeBerardinis RJ. Understanding the Intersections between Metabolism and Cancer Biology. *Cell.* 2017;168:657-669.
26. Elliott IA, Dann AM, Xu S, et al. Lysosome inhibition sensitizes pancreatic cancer to replication stress by aspartate depletion. *Proc Natl Acad Sci USA.* 2019;116:6842-6847.
27. Lane AN, Fan TW. Regulation of mammalian nucleotide metabolism and biosynthesis. *Nucleic Acids Res.* 2015;43:2466-2485.
28. Longley DB, Harkin DP, Johnston PG. 5-fluorouracil: mechanisms of action and clinical strategies. *Nat Rev Cancer.* 2003;3:330-338.
29. Quinn JJ, Chang HY. Unique features of long non-coding RNA biogenesis and function. *Nat Rev Genet.* 2016;17:47-62.
30. Gray LR, Tompkins SC, Taylor EB. Regulation of pyruvate metabolism and human disease. *Cell Mol Life Sci.* 2014;71:2577-2604.
31. Wang X, Li Y, He M, et al. UbiBrowser 2.0: a comprehensive resource for proteome-wide known and predicted ubiquitin ligase/deubiquitinase-substrate interactions in eukaryotic species. *Nucleic Acids Res.* 2022;50:D719-D728.
32. Ranek MJ, Oeing C, Sanchez-Hodge R, et al. CHIP phosphorylation by protein kinase G enhances protein quality control and attenuates cardiac ischemic injury. *Nat Commun.* 2020;11:5237.
33. Pratt WB, Gestwicki JE, Osawa Y, Lieberman AP. Targeting Hsp90/Hsp70-based protein quality control for treatment of adult onset neurodegenerative diseases. *Annu Rev Pharmacol Toxicol.* 2015;55:353-371.
34. Ajani JA, Abramov M, Bondarenko I, et al. A phase III trial comparing oral S-1/cisplatin and intravenous 5-fluorouracil/cisplatin in patients with untreated diffuse gastric cancer. *Ann Oncol.* 2017;28:2142-2148.
35. Iwashyna TJ, Lamont EB. Effectiveness of adjuvant fluorouracil in clinical practice: a population-based cohort study of elderly patients with stage III colon cancer. *J Clin Oncol.* 2002;20:3992-3998.
36. Hong YS, Song SY, Lee SI, et al. A phase II trial of capecitabine in previously untreated patients with advanced and/or metastatic gastric cancer. *Ann Oncol.* 2004;15:1344-1347.
37. Van Cutsem E, Boni C, Tabernero J, et al. Docetaxel plus oxaliplatin with or without fluorouracil or capecitabine in metastatic or locally recurrent gastric cancer: a randomized phase II study. *Ann Oncol.* 2015;26:149-156.
38. Sang B, Zhang YY, Guo ST, et al. Dual functions for OVAAL in initiation of RAF/MEK/ERK prosurvival signals and evasion of p27-mediated cellular senescence. *Proc Natl Acad Sci USA.* 2018;115:E11661-E11670.
39. Zhang J, Fan J, Venneti S, et al. Asparagine plays a critical role in regulating cellular adaptation to glutamine depletion. *Mol Cell.* 2014;56:205-218.
40. Koendjbiharie JG, van Kranenburg R, Kengen SWM. The PEP-pyruvate-oxaloacetate node: Variation at the heart of metabolism. *FEMS Microbiol Rev.* 2020;45:fuaa061.

41. Sommer H, Santi DV. Purification and amino acid analysis of an active site peptide from thymidylate synthetase containing covalently bound 5-fluoro-2'-deoxyuridylate and methylenetetrahydrofolate. *Biochem Biophys Res Commun.* 1974;57:689-695.

42. Santi DV, McHenry CS, Sommer H. Mechanism of interaction of thymidylate synthetase with 5-fluorodeoxyuridylate. *Biochemistry.* 1974;13:471-481.

SUPPORTING INFORMATION

Additional supporting information can be found online in the Supporting Information section at the end of this article.